

Submitting author/paper information: CONTRIBUTED article

Diamond 2004 PRESENTATION NUMBER: AB-154 PR

Corresponding author name: **Neidenêi Gomes Ferreira**

Mailing address:

Laboratório Associado de Sensores e Materiais – LAS

Instituto Nacional de Pesquisas Espaciais

Av. dos Astronautas, 1758

Jd. Da Granja

CEP. 12245-970

São José dos Campos, S.P., Brasil

Fax number: +55 12-3945-6717

Telephone number: +55 12-3945-6675

E-mail: neidenei@las.inpe.br

Title: Doctor

Keywords: carbon fibers, diamond films, doping p-type, electrode arrangement

Estimated word count: 4216 words

Prime Novelty: The influence of heat treatment temperature (HTT) on the carbon felts structural properties and its relation with diamond film properties and electrochemical response.

“The submission of the manuscript has been approved buy all co-author(s).”

Structural and voltammetric studies at boron-doped diamond electrode grown on carbon felt produced from different temperatures

E. C. Almeida¹, A. V. Diniz^{1,2}, J. M. Rosolen³, V.J. Trava-Airoldi¹ and N. G. Ferreira¹

¹INPE - C. P. 515 - 12201-970 - São José dos Campos, S.P., Brasil

²ITA, 12228-900, São José dos Campos, SP, Brasil

³DQ, FFCLRP, Universidade de São Paulo, 14040-901 Ribeirão Preto, SP, Brazil

erica@las.inpe.br; neidenei@las.inpe.br

Diamond formation was studied on carbon felts (CF) substrates produced from an organic polymer, polyacrylonitrile (PAN), at different heat treatment temperatures (HTT). CF structural properties knowledge and control have demonstrated to be very important for growing boron-doped diamond (BDD) films on such substrates. During the deposition, fiber etching and diamond nucleation occur simultaneously and compete kinetically. In addition, these processes may also be affected by the HTT of the carbon fiber precursor. BDD/CF electrodes were produced by Hot Filament Chemical Vapor Deposition (HFCVD) and characterized by Scanning Electron Microscopy (SEM), Raman spectroscopy, X-Ray Diffraction (XRD) and Cyclic Voltammetry (CV) techniques. It is also discussed the HTT influence on substrate structural properties correlated with diamond film growth and its electrochemical response. CF substrates were carburized in the temperatures of 1300, 1800 and 2300 K and presented representative increase in their conductivity values. CV measurements in ferri-ferrocyanide system have confirmed the superior properties of

BDD/CF electrodes and evidenced a large surface area increase, which turns them appropriate to be used as porous electrode in different electrochemical applications.

1. Introduction

Carbon fibers are new breed of high-strength materials and have been described as a fiber containing at least 90% carbon obtained by the controlled pyrolysis of appropriate fibers. Numerous precursors are used for producing carbon fibers such as cotton, linen, ramie, sisal and flax. However, the main three precursors used for large-scale production of carbon fibers are PAN, rayon, and pitches [1]. PAN based fibers present superior physical properties compared to rayon-based fibers [2]. Besides, the fabrication process is easier and more economical due to higher carbon yield, which is 50% against 30% for rayon [3].

Many properties of PAN-based carbon fibers may be affected by their production process. The carbonization rate, and consequently the produced gases, must be controlled to prevent defects in the fibers. Pores are created in the fiber owing to the formation and perfection of carbon layer structures. The high temperature in carbonization process increases the crystalline perfection of the fibers and become more perfect the carbon layer planes, generating a large closed pore structure [1]. The electric conductivity is strongly affected by HTT increase. In recent studies it was observed that electric conductivity values increase up to 1800 K and keep almost constant up to 2300 K [4].

Considering the numerous electrochemical applications of carbon-based electrodes, a constant search of developing new materials represents a challenge. Besides, it is fact their importance for surface processes, which require durability and efficiency. The frequent use of carbon electrodes in electrochemical applications [5-7] makes the

production of diamond films on CF substrates an alternative procedure for increasing the lifetime and electrode superficial area. In addition, the conductivity control of diamond films through the boron doping level control may guarantee a suitable electrode keeping its necessary chemical inertness [8].

Diamond growth mechanisms on carbon fibers have already discussed by some authors [9-11]. It is known that diamond deposition on carbon substrates using low-pressure techniques may be unfavorable due to atomic hydrogen etching. The authors generally accept that super saturation of hydrogen enhances the diamond formation and suppresses the formation of non-diamond phases. Angus and co-workers [12] have reported diamond nucleation on graphite and suggested that the graphite surface itself acts as a nucleation center in the atomic hydrogen presence.

The main purpose of this study is production and characterization of boron-doped diamond electrode grown on carbon felt (BDD/CF) by using Raman spectroscopy, XRD and CV techniques. It is also discussed HTT influence on substrate structural properties related with diamond film growth and its electrochemical response.

2. Experimental

CF samples were produced from PAN at different HTT by using temperature steps of 330 K/h under inert atmosphere (nitrogen flow of 1 L.h⁻¹), reaching maximum temperature of 1300, 1800 and 2300 K. The maximum temperature was maintained for 30 min and after cooled down to room temperature. The samples are denoted CF-1300, CF-1800, CF-2300 and consist of felt disks with 0.15 cm thickness and 1.8 cm diameter.

BDD films were grown by HFCVD technique during 20 hours from 0.5% CH₄/H₂ mixture. The substrate temperature and total pressure were 1050 K and 6.5 x 10³ Pa, respectively. The substrates were ultrasonically pre-treated in a mixture of 0.25 μm diamond powder and hexane. Boron source was obtained from H₂ line forced to pass through a bubbler containing B₂O₃ dissolved in methanol. This system permits the control of boron concentration in the films using a flow controller. The doping level used (5000 ppm B/C in methanol) corresponds to acceptor concentration of 1.5 x 10¹⁸ cm⁻³, evaluated by Mott-Schottky Plot measurements in previous work [8] and correlated with Raman spectra [13].

Samples were kept in the vertical position inside the reactor between two pairs of parallel tungsten filaments that permitted film growth on both sides, simultaneously. This procedure is important to guarantee diamond growth over all carbon fibers, including that ones in deeper planes. Top view and cross-section images of BDD/CF films were obtained by SEM from a Jeol equipment JSM-5310. Micro-Raman spectra were recorded by a Renishaw microscope system 2000 in backscattering configuration. CV measurements were carried out using a potentiostat Omnimetra Instrumentos PG 3901 for BDD/CF and CF electrodes at different HTT. The electrode geometric superficial area exposed in solution was 5.0 cm², considering both sides and thickness of sample (as a three dimensional electrode). The anodic and cathodic charges were evaluated from VC curves obtained in 1 mM ferrocyanide/0.1M KCl at scan rates from 5 to 500 mV/s. The experiments were conducted at room temperature. Simple three-electrodes (work, Ag/AgCl and platinum electrode) in a single-compartment electrochemical cell was used in this study. The electrodes did not undergo surface treatment before the electrochemical measurements.

3. Results and discussion

3.1. CF Structural Characterization

During thermal treatment, most of the non-carbon elements within the fibers are volatilized in form of methane, hydrogen, hydrogen cyanide, water, carbon monoxide, carbon dioxide, ammonia and various other gases [14,15].

The evolution of these compounds decreases the fiber mass 55-60 wt% [16]. As a result, the fiber diameter shrinks. Therefore, in a typical PAN process, the precursor fiber might have a diameter of 35 μm and after carbonization the final fiber 10 μm . In this range of HTT it was not observed a stretched of the fibers diameter, but an increase of tensile strength [17,18]. The average values of CF diameters obtained from SEM images are shown in Table 1 as a function of HTT. The fibers diameter values are around 10 μm and does not show a significant variation according to the literature.

Micro-structural properties of PAN-based CF are strongly affected by HTT and can influence the diamond nucleation and growth as well as the BDD/CF electrochemical response. In addition, HTT influences the electrical properties because there is a preferential orientation increase of graphitic sheets in fiber axial direction at higher temperature. The resistivity values (ρ) observed in Tab.1 were evaluated through four-probe method and are in good agreement with the literature [4]. Besides, the values present lower average standard deviation. At 2300 K the value decreases almost 8 times compared with sample treated at 1300 K. Table 1 also presents, for the three HTT studied, other CF experimental parameters: pilling up width of layers (L_{002}) and interlayer distance (d_{002});

FWHM ratio (ω_D/ω_G) and the relative intensity (I_D/I_G) between the D and G bands, obtained from XRD and Raman spectra, respectively [4,19].

The interlayer distance calculated from (002) bands decreases with HTT increase but is larger than graphitizable cokes (3.44 Å) treated above 1300 K [20]. This behavior supports the arguments that the carbon layers are highly strained and the internal strain energy did not release with the HTT. The carbon layers in the crystallites are apparently compressed along the basal plane and bent due to the surrounding crystallites.

CF first-order Raman spectra display two dominant bands called G and D. The G-band occurs between 1575 and 1600 cm^{-1} due to E_{2g} vibration mode in ordered graphitic structure [21]. The D-band can be found at 1355-1360 cm^{-1} , and it is a good indication of the crystal structure disorder. D-bands are associated to discontinuation of hexagonal carbon layer planes [21,22]. The results from first-order Raman spectroscopy (Tab.1) seem to be in agreement with those of XRD; ω_D/ω_G and I_D/I_G decrease with HTT increase, revealing the CF graphitization at 2300K.

3.2. Diamond Surface Morphology and Raman Analysis

The main difficulty of growing diamond films on graphite is sp^2 -bond etching on substrates caused by atomic hydrogen presents in gas phase, which is the main precursor for diamond growth. Substrate pre-treatment is necessary to improve the diamond growth on carbon substrates keeping the carbon surface in dominant sp^3 configuration over reconstruction into graphitic sp^2 configuration [23-25]. SEM image of diamond film on CF-2300 sample, with a doping level of around 10^{18} atoms.cm^{-3} , is showed in Fig.1a and

demonstrates CF surface completely covered by diamond polycrystalline film. The grains are faceted with symmetrical and smooth faces evidencing a uniform texture and dominant (111) type planes. The average grain sizes were also evaluated in 3.0 and 6.0 μm for CF-1300 and CF-2300, respectively.

Diamond coating presented thickness of approximately 3.0 μm , as can be observed in Fig 1b. This value decreases for internal fibers, as expected, taking into account the critical depth for diamond formation, which is mainly related to atomic hydrogen diffusion mechanisms. SEM cross-section image obtained in sample center region still evidences diamond film existence. This verification is important for electrochemical applications by considering these samples as three-dimensional electrodes that also need to have inner fibers covered by diamond film. Electrode superficial texture is directly related to electrode active area and, consequently, electrochemical response.

The quality of BDD/CF electrodes were studied by Raman spectroscopy. Figure 2 shows Raman spectra for BDD/CF-1300 (a), BDD/CF-1800 (b) and BDD/CF-2300 (c). Raman spectra evidenced sharp 1332 cm^{-1} peak, indicating films constituted mainly by diamond crystals. In addition, a broad band centered on 1550 cm^{-1} appeared in (a) and (b) curves. This band is attributed to disordered graphitic phases and disappears in (c) curve. This is probably associated to the best CF structural organization at higher HTT. During higher carbonization temperature, the fibers crystalline quality increases and carbon layer planes become more perfect, generating a larger close pore structure [1].

3.3. Electrochemical Behavior

CV has demonstrated to be an easy and fast method to study electrochemical response of electrode surface. Several works have presented important studies employing this technique for BDD electrodes [26-30]. This work presents preliminary electrochemical analyses of BDD/CF electrodes as a function of substrate HTT. The main objective is to compare how electrochemical response can be influenced by changes observed in substrate structure and film morphology.

The treatment of systems called quasi-reversible is associated to reactions that show electrons transfer kinetic limitations and consequently for these systems reverse reactions have to be considered. The results presented in previous works have led us to conclude this is the most suitable treatment for BDD/CF electrodes in the studied redox system. In this way, BDD/CF electrodes were analyzed by the quasi-reversibility criteria: the separation between the anodic and cathodic peaks (ΔE_p) is larger than $59/n$ mV (where $n = 1$ is the number of electrons involved in the reaction) and increases with sweeping rate (ν) increase; current peak intensity (I_p) increases with $\nu^{1/2}$ increase, but does not keep proportionality; and the cathodic peak potential (E_{pc}) shifts to negative values, with ν increase [31]. The usual reduction and oxidation current peaks were exhibited for all electrodes studied using ferro/ferrocyanide redox couple. Besides, the kinetic parameters analyses were studied as a function of substrate HTT. Electrochemical response also permitted to evaluate electrode Specific Electrochemical Surface Area (SESA).

The substrate effect on the reported electrochemical experiments may be discussed from curves obtained in 1mM of ferrocyanide/0.1M KCl at $\nu = 50$ mV/s and presented in

Fig. 3. Curve (a) represents the CF electrode response while curve (b) shows response for BDD/CF electrode. Both CF samples were carbonized at 2300 K. The predominant substrate contribution is related to smaller ΔE_p for CF electrode (270 mV) when compared to BDD/CF electrode ΔE_p (530 mV). This behavior is attributed to CF conductivity that becomes less dominant when doped diamond covers carbon fibers and electrode conduction is controlled by boron doping level. Besides, the higher current density for curve (b) is attributed to polycrystalline diamond surface texture, with higher roughness, that defines higher active electrochemical area and capacitance.

By considering the non-Faradaic contribution, CF electrodes present higher background current mainly due to their higher active electrochemical area, like usually observed on carbonaceous porous electrodes [32]. On the other hand, an important property of diamond electrode is low background current (two orders of magnitude lower than glass carbon electrode) [33]. We can speculate that there is not an inconsistency of growing diamond on CF substrates; in spite of the film to promote a higher active area. Even for detecting small quantities of chemical species in electroanalytical applications, it is possible to keep the higher sensitivity of BDD/CF electrode. The higher anodic or cathodic peak current, produced by such analyzed species, easily compensates its background current.

Figure 4 presents CV curves at 50 mV/s for BDD/CF electrodes that correspond to diamond films grown on substrates of 1300, 1800 and 2300 K HTT. It is possible to note there are variations on ΔE_p values and active electrochemical area, so these parameters were detailed studied. In the Fig. 5, ΔE_p values were also represented as a function of ν . ΔE_p , which is larger than $59/n$ mV, increases with the ν increase for all HTT. Besides, it

was observed the ν increase promotes an increase in I_p for cathodic and anodic reactions. Therefore, according to the reversibility criteria, the systems confirm to be quasi-reversible. In addition, it is possible to observe the ΔE_p values are higher for the lower HTT. This behavior is in agreement with resistivity values discussed in Tab.1. The higher electrical conduction of the BDD/CF-1800 and 2300 electrodes improves the electron transfer in electrochemical experiments and decreases ΔE_p .

SESA values were calculated by the equation [34]:

$$\text{SESA} = \frac{I_p}{2,69 \times 10^5 C_o V_{el} \sqrt{D_o \nu}},$$

where I_p is anodic peak current intensity (A), C_o is oxidant concentration (mol/L, equal to reductor), V_{el} is electrode volume immersed in solution (cm^3), D_o is oxidant diffusivity in solution (cm^2s^{-1} , it is also considered equal to reductor), and ν is sweeping rate (Vs^{-1}).

SESA of BDD/CF electrodes were evaluated from the curves presented in Fig.4. The found values were 540, 400 and 330 cm^2 , for 1300, 1800 and 2300 K HTT, respectively. This result may be related to surface morphologies observed by SEM. However, in the case of three-dimensional porous electrode, like BDD/CF, different contributions should be considered. First of all, the film grows around the fibers increasing their diameters and the superficial area of each fiber. For higher growth rates, larger grain size and roughness are expected, which can also promote a larger SESA. At the same time, the contributions from films with larger grain size and fibers with larger diameter tend to fill empty spaces between the fibers. This process consequently decreases the porosity associated to active electrochemical area and it seems to be more relevant for BDD/CF-2300 electrode.

4. Conclusion

BDD films were grown on CF, which were produced at different HTT, with good quality and adherence. SEM images show all grains faceted, with symmetrical and smooth faces. A variation in average grain size was also observed: 3.0 and 6.0 μm for BDD/CF-1300 and BDD/CF-2300, respectively. Diamond coating have presented a thickness of approximately 3.0 μm . CF structural characterization revealed a very large interlayer spacing, calculated from (002) bands, and much smaller apparent crystallites sizes if compared to graphitizing carbons. The results from first order Raman spectroscopy are in good agreement with those obtained from XRD: $\omega_{\text{D}}/\omega_{\text{G}}$ and $I_{\text{D}}/I_{\text{G}}$ decrease with HTT increase revealing graphitization for CF at 2300K HTT.

The polycrystalline diamond surface texture, with higher roughness, defines higher active electrochemical area and capacitance. However, BDD/CF electrode can detect small quantities of chemical species, keeping the higher sensitivity, once the higher anodic or cathodic peak current can easily compensate its background current. The ν increase promotes an increase in the I_p and ΔE_p for all HTT, confirming the quasi-reversible systems. The substrate effect on the electrochemical results can be observed through CF conductivity that becomes less dominant when conduction is controlled by boron doping level in BDD/CF electrodes. The electrochemical response is influenced by changes observed in substrate structure and film morphology as observed in the following results. ΔE_p values are higher for the lower HTT in agreement with higher CF resistivity values. SESA values for BDD/CF electrodes has demonstrated high electrochemical active area, which makes them very promising for applications as electrochemical capacitor. However,

there are two contributions of diamond film: the film growth around the fibers increasing their diameters, roughness and the superficial area of each fiber; and fibers with larger diameter tend to fill empty spaces between the fibers decreasing the porosity and active electrochemical area.

Acknowledgements

The authors would like to thank CNPq (Process 300699/2003-4) and FAPESP (Processes n° 01/11619-4 and 02/03744-6) by the financial support and Mrs. M.L. Brison by SEM analyses.

References

- [1] L.H. Peebles, “ Carbon Fibers: Formation, Structure, and Properties”, CRC Press, Florida, 1995.
- [2] S. Chand, Journal of Materials Science 35 (2000) 1303.
- [3] E. Fitzer, *ibid.* 27 (1989) 621.
- [4] J.K Lee, K.W An, J.B Ju, B.W. Cho, W. Cho, D.Park, K. S. Yun, Carbon 39 (2001) 1299
- [5] R. Ramesham, Thin Solid Films 339 (1999) 82.
- [6] X.-X Yan, D-Wen Pang, Z-X Lu, J.-Q Lü and H. Tong, J. Electroanal. Chem. 569 (2004) 47 .
- [7] J. M. Friedrich, C. Ponce-de-León, G. W. Reade, F. C. Walsh, J. Electroanal. Chem. 561 (2004) 203.

- [8] N.G. Ferreira, L.L. G. Silva, E.J. Corat, V.J. Trava-Airoldi ,Diamond Relat. Mater. 11 (2002) 1523.
- [9] S.I. Shah, M.M. Waite, J. Vac. Sci. Technol. A 13 (1995) 1624.
- [10] J. Tin and M. L. Lake, J. Mat. Res. 9 (1994) 636.
- [11] P.E. Pehrsson, J. Glesener and A. Morrish, Thin Solid Films 212 (1992) 81.
- [12] Z. Li, L. Wang, T. Suzuki, A. Argoitia, P. Pirouz and J. C. Angus, J. Appl. Phys. 73 (1993) 711.
- [13] R.J. Zhang, S.T. Lee, Y.M. Lam, Diamond Relat. Mater. 5 (1996) 1288.
- [14] W. Turner, J. Appl. Polymer Sci. 9 (1968) 1245.
- [15] J.E. Bailey, A. J. Clarke, Nature 234 (1971) 529.
- [16] D.D. Edie, Carbon 36 (1998) 621.
- [17] J-B. Donnet, R.C. Bansal, Carbon Fibers, Marcel Dekker INC., New York, 1990.
- [18] E. Fitzer, Carbon, 27 (1989) 621.
- [19] S.R. Dhakate, O. P. Bahl, Carbon 41 (2003) 1193.
- [20] G.M Jenkins, K. Kawamura, Polymeric carbons- carbon fibre, glass and char, Cambridge University Press, Cambridge, 1976, p.52.
- [21] R.J Nemanich, S. A. Solin, Phys. Rev. B 20 (1979) 392.
- [22] G. Katagiri, H. Ishida, Carbon 26 (1988) 565.
- [23] J. Ting, M.L. Lake, J. Mater. Res. 9 (1994) 636.
- [24] S.I. Shah, M.M. Waite, J. Vac. Sci. Technol. A 13 (1995) 1624.
- [25] E. Johansson, A.S Norekrans, J.O. Carlsson, Diamond Relat. Mater. 2 (1993) 383.
- [26] G.M. Swain and R. Ramesham. *Anal. Chem.* 65 (1993) 345.
- [27] G.M. Swain, *J. Electrochem. Soc.* 141 (1994) 3382.
- [28] R. Ramesham and M.F. Rose, *J. Mater. Sci. Lett.* 16 (1997) 799.

- [29] K. Patel, K. Hashimoto, and A. Fujishima, *J. Photochem. Photobiol., A: Chem.* 65 (1992) 419.
- [30] Yu.V. Pleskov, V.V. Elkin, M.A. Abaturon, M. D. Krotova, V. Ya Mishuk, V. P. Varnun, I.G. Teremetskaya, *J. Electroanal. Chem.* 413 (1996) 105.
- [31] R. Greef, R. Peat, L. M. Peter, D. Pletcher, J. Robinson, *Instrumental Methods in Electrochemistry*, ch. 6, Wiley, New York, 1985.
- [32] C. A. Frysz, X. Xhui, D.D.L. Chung, *Carbon* 35 (1997) 893.
- [33] R.C. Mendes de Barros, N.G. Ferreira, E.J. Corat, S.H.P. Serrano. *J. Braz. Chem. Soc.* *in press.*
- [34] S. Trassatti, O. A Petrii, *Pure Appl. Chem.* 5 (1991) 711.

Figure Captions

Table 1. PAN-CF parameters at different HTT obtained by four-probe method, SEM, XRD and first order Raman spectroscopy.

Figure 1. SEM images of diamond film grown on CF-2300, with a doping level of 10^{18} atoms.cm⁻³ B/C: (a) morphology and (b) cross section evidencing diamond film thickness.

Figure 2. Raman spectra of diamond films: (a) BDD/CF-1300, (b) BDD/CF-1800 and (c) BDD/CF-2300.

Figure 3. Voltammetric curves in 1mM ferrocyanide/0.1M KCl at 50 mV/s: (a) CF-2300 and (b) BDD/CF-2300 electrodes.

Figure 4. Voltammetric curves in 1mM ferrocyanide/0.1M KCl at 50 mV/s for BDD/CF-1300, BDD/CF-1800 and BDD/CF-2300 electrodes.

Figure 5. ΔE_p as a function of sweeping rate in 1mM ferrocyanide/0.1M KCl for BDD/CF-1300, BDD/CF-1800 and BDD/CF-2300 electrodes.

HHT (K)	CF diameter (μm)	ρ ($\Omega\cdot\text{cm}$)	d_{002} (\AA)	L_{002} (\AA)	ω_D/ω_G	I_D/I_G
1300	10.4 ± 0.3	0.96 ± 0.39	4.34	11.6	2.76 ± 0.40	0.98 ± 0.02
1800	10.4 ± 0.14	0.11 ± 0.01	4.25	16.2	1.51 ± 0.38	0.79 ± 0.15
2300	10.07 ± 0.22	0.11 ± 0.006	4.16	23.1	0.92 ± 0.01	0.73 ± 0.05

Table 1

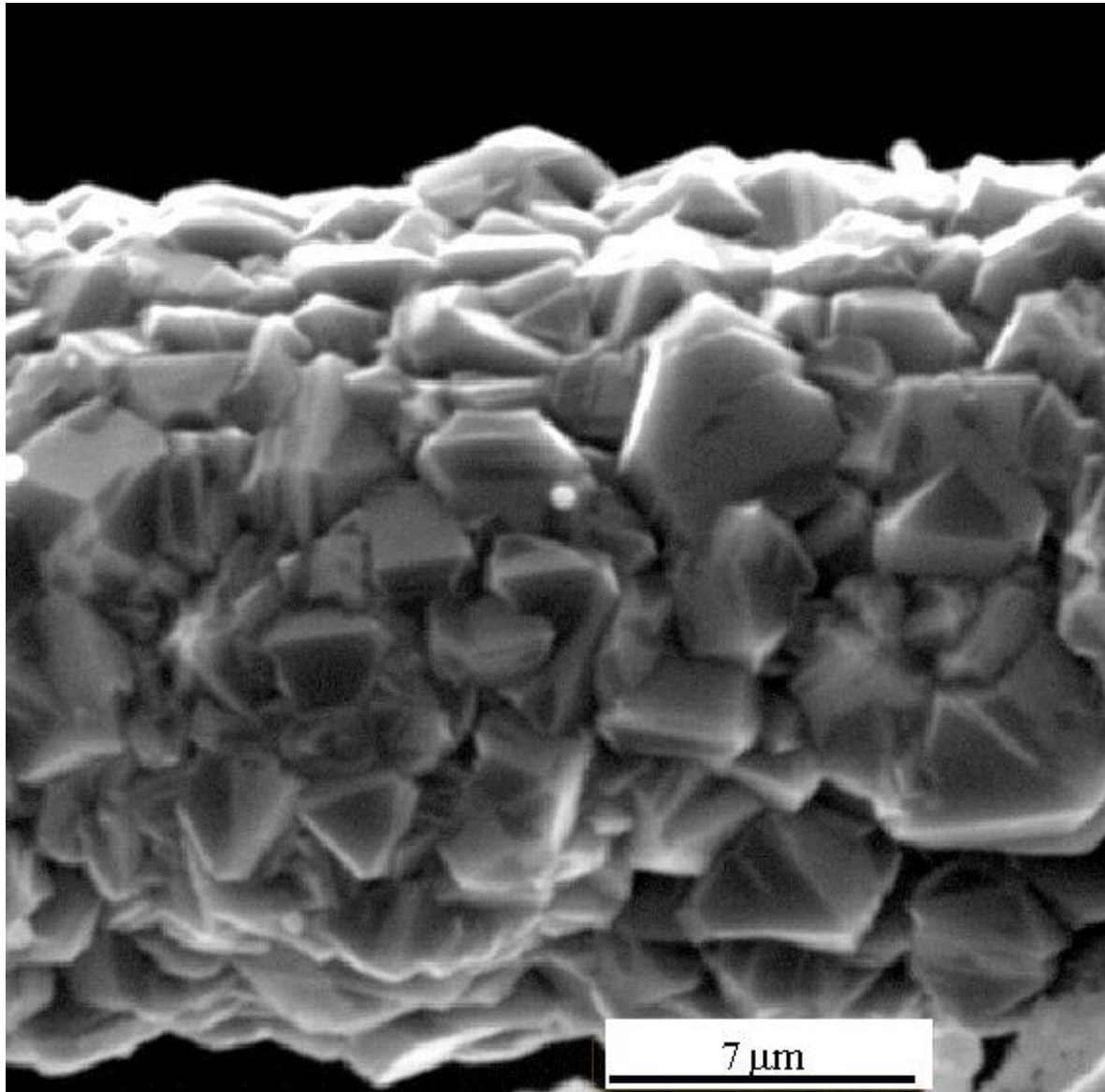


Figure 1a

Re

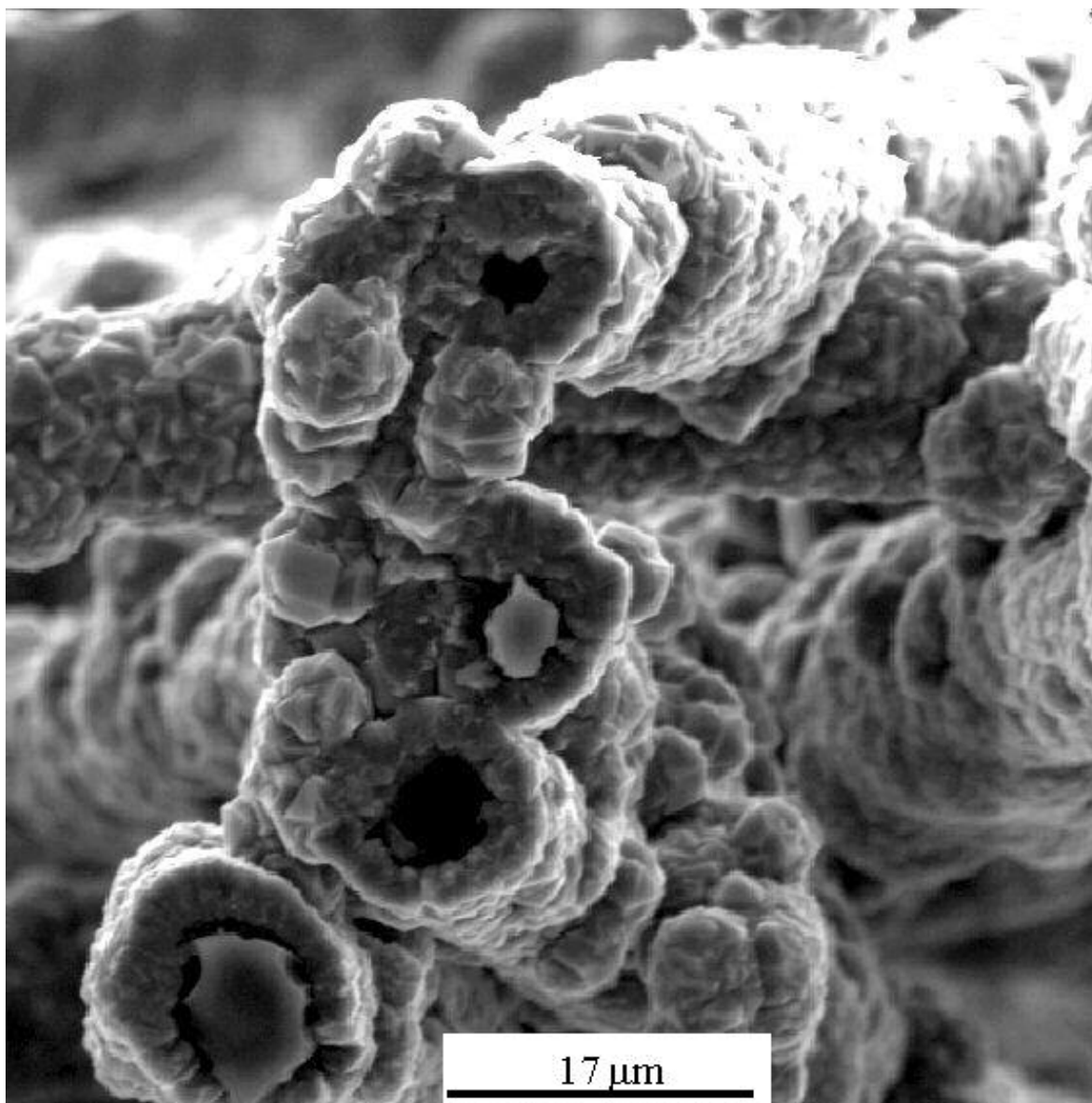


Figure 1b

Review

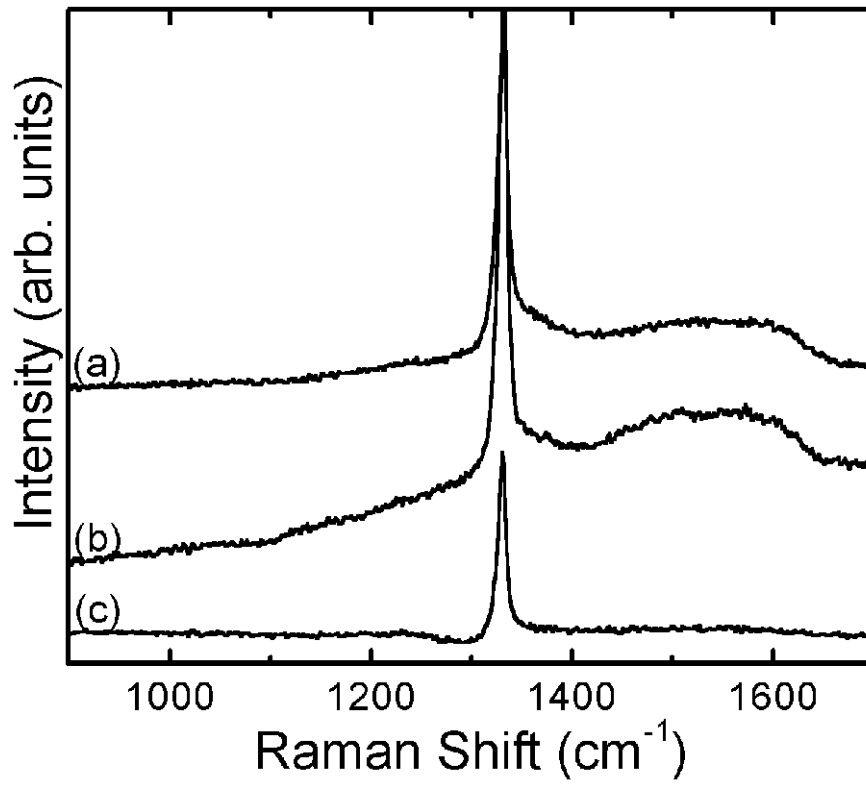


Figure 2

Review

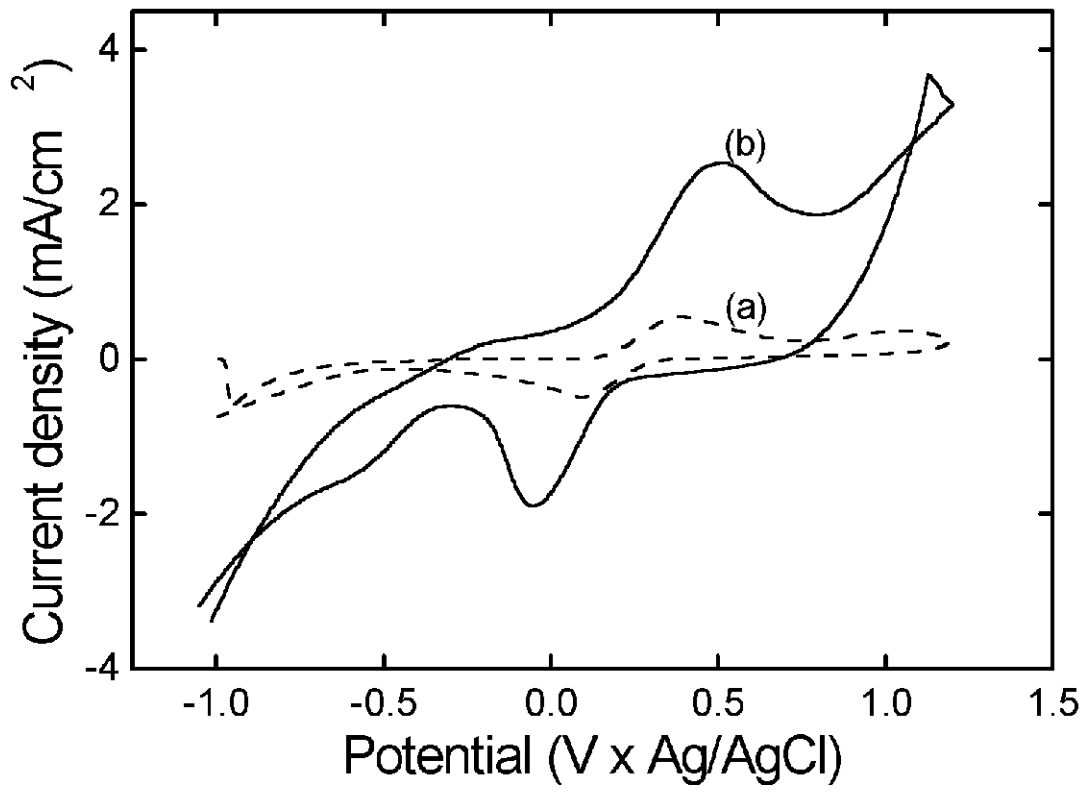


Figure 3

Review

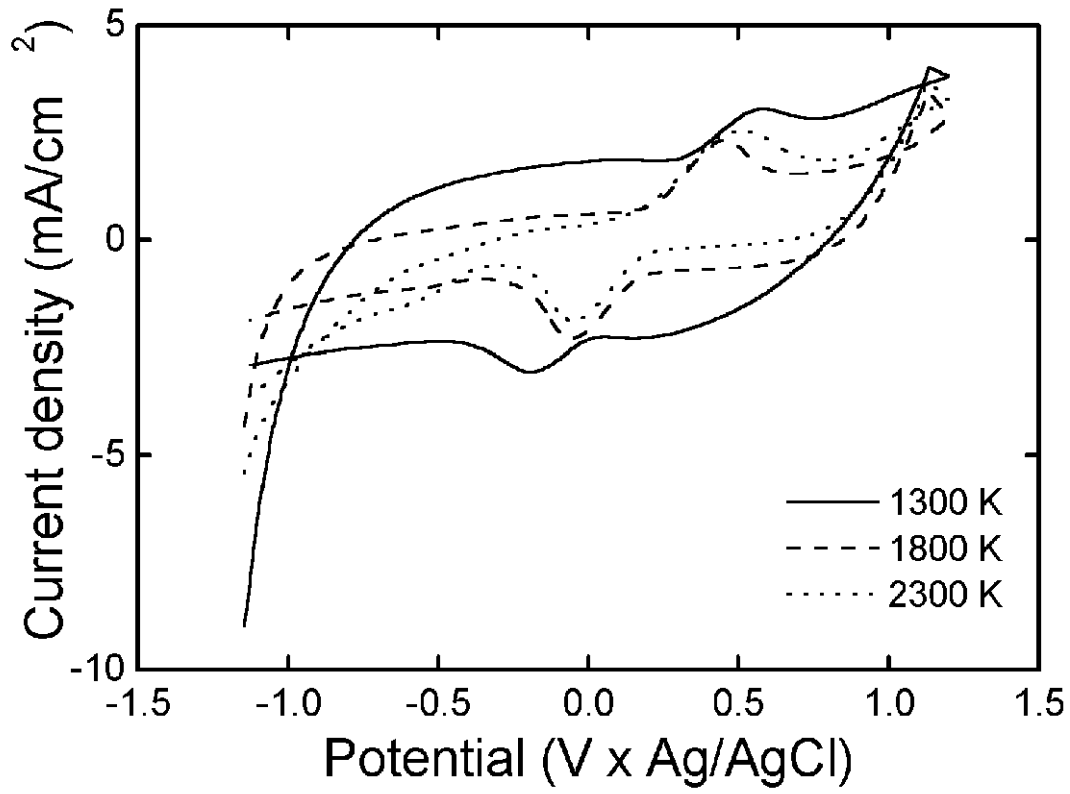


Figure 4

Review

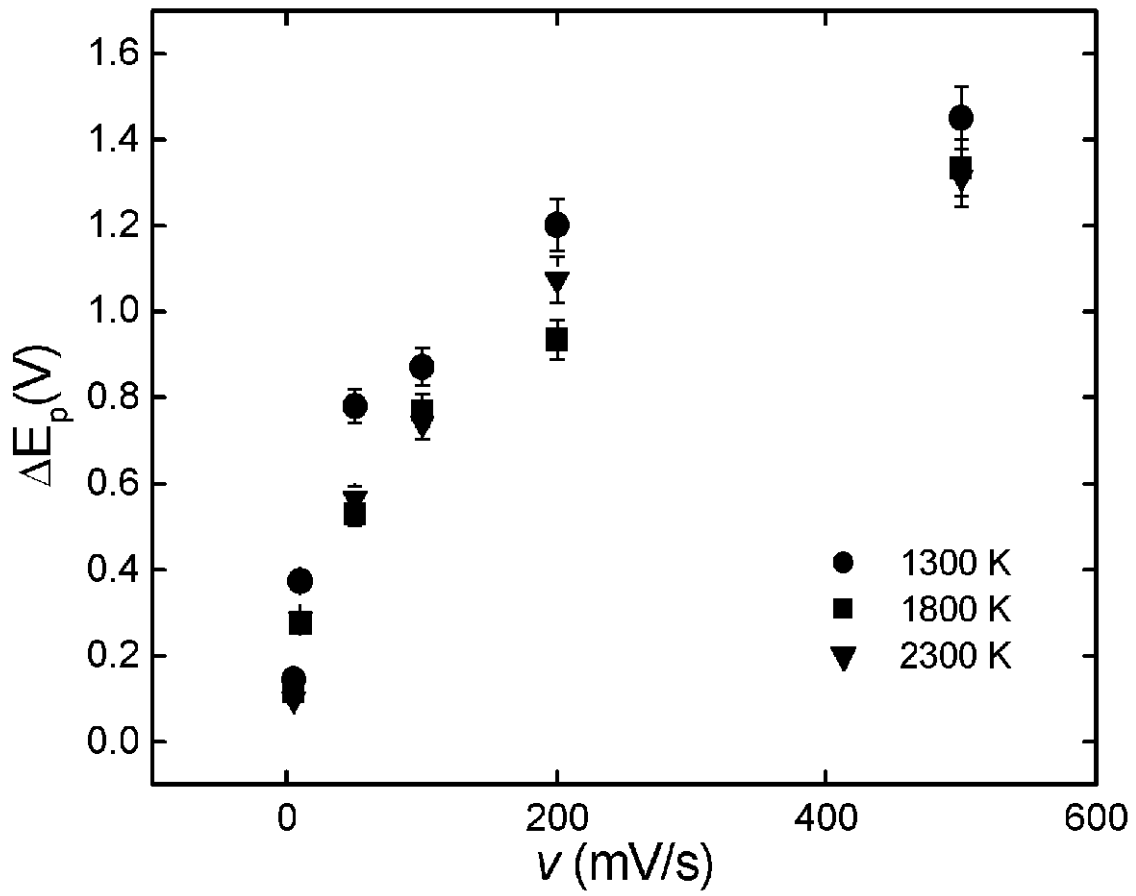


Figure 5

Review